

Generalized Lindemann Melting Law

Marvin Ross

Lawrence Radiation Laboratory, University of California, Livermore, California 94550

(Received 20 January 1969)

The Lindemann melting law is generalized by reformulating it in terms of the statistical-mechanical partition function. With the reformulated law, a melting curve is calculated for argon, which is in good agreement with experiment. A number of well-known melting laws are derived by using this generalized approach.

I. INTRODUCTION

One of the oldest and most widely used attempts to predict the melting curves of solids is that due to Lindemann.¹ Lindemann assumed that a solid melts when the mean-square amplitude of vibrations of atoms about their equilibrium position becomes larger than a certain fraction of the lattice spacing. He then straightforwardly arrived at a relationship between the melting temperature T_m , the melting volume v_m , and the force constant of the oscillator.

The purpose of this paper is to present a reformulation of Lindemann's approach from a more general statistical-mechanical point of view so that it may be applicable to any functional form of the intermolecular potential. Section II presents this reformulation in terms of the partition function, and as an application, in Sec. III an intermolecular potential of the van der Waals type is used to calculate the thermodynamic properties along the melting curve for argon. In Sec. IV, it is shown that Lindemann's Law, the Simon equation,² and the melting law recently proposed by Kraut and Kennedy³ all follow from this generalized Lindemann point of view.

The Lindemann approach to melting is a one-phase theory. It only treats the solid and says nothing about the liquid or why the solid becomes a liquid. Since it does not present a mechanism for melting, it is not truly a theory of melting. Instead, it evolves from an intuitive sense of what must be occurring. The results of this paper appear to further justify this intuition.

II. FORMULATION OF GENERALIZED LINDEMANN MELTING CRITERIA

In this section, the Lindemann approach to melting will be generalized in terms of a statistical-mechanical formalism. In statistical mechanics, the configurational partition function Q for a system of N particles is written

$$Q = (1/N!) \int \cdots \int \exp[-U(\bar{r}_1, \bar{r}_2, \cdots, \bar{r}_N) \beta] \times d\bar{r}_1 d\bar{r}_2 \cdots d\bar{r}_N.$$

Defining a set of reduced coordinates $\bar{\lambda} = \bar{r}/V^{1/3}$, where V is the volume of the entire system, we may rewrite the configurational partition function in terms of a reduced configurational partition function Q^* .

$$Q = (V^N/N!) \int \cdots \int \exp\{-[U(\bar{\lambda}_1, \bar{\lambda}_2, \dots, \bar{\lambda}_N) - U(0)] \beta\} d\bar{\lambda}_1 \cdots d\bar{\lambda}_N e^{-U(0)\beta},$$

$$Q = V^N Q^* [e^{-U(0)\beta}/N!],$$

$$Q^* = \iint e\{-[U(\bar{\lambda}_1, \bar{\lambda}_N) - U(0)] \beta\} d\bar{\lambda}_1 \cdots d\bar{\lambda}_N,$$

where $U(0)$ is the energy of the system with all atoms at their lattice sites, and Q^* is an integral over the reduced configuration space and can be thought of as a measure of the fraction of this space available to the system.

The Lindemann approach to melting takes the view that if we were able to see the melting transition on a microscopic level, we would always see the same scaled picture in the solid. At different temperatures, because of their ability to interpenetrate each other's electronic cores, the atoms will have different effective sizes. However, for a given crystal structure, the ratios of their effective volumes to the total volume of the system will always remain constant at all points along the melting curve, and their relative arrangements in space will always remain the same. Consequently, the pictures along the melting curve will always be identical if properly scaled. We wish to generalize this point of view which is expressed in terms of real space into terms of statistical mechanics by reexpressing Lindemann's Law in terms of configurational space.

The Lindemann principle is reformulated by stating that for a given substance, at all points along its melting curve, the solid always occupies the same fraction of configurational phase space. In other words, in configurational space we would always see the same scaled picture at all points along the melting curve. In statistical-mechan-

ical language we require that Q^* be a constant at all melting temperatures T_m and all volumes V_m along the melting curve, and this is formally written

$$Q^*(T_m, V_m) = \text{const.}$$

One of the advantages of formulating Lindemann's Law in terms of the partition function is that it is this quantity that provides us with a direct link to all of the thermodynamic properties of the system in a straightforward way. Unfortunately, this formulation in terms of the total partition function Q is too general to be useful in simple calculations, and, therefore, it becomes necessary to choose a model for a solid. In this paper, we will choose the single-particle cell model. In the cell model the volume V is divided up into a lattice of N cells with one molecule in each cell. Each molecule is confined within its cell and moves in the potential field of its neighbors, but its motion is independent of its neighbors. In the single-particle cell-model approximation, the configurational partition function now denoted as $Q^{(1)}$ may be written⁴

$$Q^{(1)} = v_f^N e^{-NE(0)/2\beta},$$

where v_f is the one-particle free volume given by

$$v_f = \int_v e^{-[E(\bar{r}) - E(0)]\beta} d\bar{r}. \quad (1)$$

The integral is over v , the volume of the cell; $E(\bar{r})$ is the potential field in which the particle moves, and $E(0)$ is the potential at the center of the cell. Defining a set of reduced coordinates $\bar{\lambda} = \bar{r}/v^{1/3}$, where v is the volume of a cell enables us to express v_f as

$$v_f = v v_f^*, \quad v_f^* = \int_0^1 e^{-[E(\bar{\lambda}) - E(0)]\beta} d\bar{\lambda}, \quad (2)$$

$$\text{or } Q^{(1)} = v^N v_f^{*N} e^{-NE(0)/2\beta}.$$

Here v_f is the volume of configuration space that a single molecule wandering in its cell will occupy. Then v_f^* is the dimensionless reduced volume occupied by a single particle and is the cell-model analog of the many-particle function Q^* defined previously. Consequently, in terms of the cell model, our melting principle will be postulated as

$$v_f^*(T_m, v_m) = \text{const.} \quad (3)$$

In the configuration space of the single particle, we will always see the same scaled picture at all points along the melting curve.

The free energy is written

$$A = -kT \ln Q^{(1)}.$$

Combining with Eqs. (1) and (2) we obtain

$$A = \frac{1}{2} NE(0) - NkT \ln v - NkT \ln v_f^*, \quad (4)$$

the free energy of the solid in the single-particle cell-model approximation. Using Eq. (4) and its various derivatives we can calculate all of the thermodynamic properties along the melting curve once T_m and v_m have been determined by the application of Eq. (3). We would like to emphasize that one of the advantages of the present formalism is that it allows us to use the full intermolecular potential and not just the harmonic approximation as in the Lindemann Law.

The remainder of this paper is devoted to applying these ideas as expressed in Eqs. (3) and (4) to a few examples. Equation (3) has been derived using classical statistical mechanics in the single-particle approximation, and as a result it is applicable only to systems in which quantum effects are negligible.

III. APPLICATION TO SOLID ARGON

In this section, we illustrate the full advantage of reformulating the Lindemann principle in terms of the partition function by applying the formulation to calculating the melting curve for argon and some of the thermodynamic properties along this curve using the full form of the intermolecular potential.

Our model for the solid is the well-known Lennard-Jones-Devonshire⁵ (LJD) cell model which is a single-particle model of the solid. It has been discussed extensively by Barker⁶ who has included all of the thermodynamic relations for this model. In the LJD cell model, the atom moves in a potential field obtained by summing the pair potential over all its stationary neighbors and then taking a spherical average. This potential is used in Eq. (1), and the thermodynamic properties are derived from Eq. (4). Although this model was originally formulated as a model for the liquid, it is generally recognized to be a very good model for a molecular solid. Ross and Alder⁷ have made Monte Carlo calculations for solid argon along a 65°K isotherm using a Lennard-Jones-type intermolecular potential and showed that to within ±50 bars, the accuracy of the Monte Carlo calculations, the LJD calculations were in agreement. Since the Monte Carlo calculations are in principle exact, the LJD model may be considered as a satisfactory representation of the P, V, T space of the solid.

However, in order to test the theory and calculate the experimental melting curves, it is obviously necessary to have an intermolecular potential which will correctly reproduce the static

P , V , T measurements independent of the correctness of the melting theory. The intermolecular potential used was assumed to be pairwise additive and of the exponential-six functional form.

$$\phi(r) = \epsilon \left\{ \left(\frac{6}{\alpha - 6} \right) \exp \left[\alpha \left(1 - \frac{r}{r^*} \right) \right] - \left(\frac{\alpha}{\alpha - 6} \right) \left(\frac{r^*}{r} \right)^6 \right\}. \quad (5)$$

The parameters r^* , ϵ , and α were obtained by using the potential in the LJD model to find those values of the parameters for which the LJD model best reproduced the static data that had been measured in P , V , T space near the melting curve. No attempt has been made to obtain detailed agreement by an exhaustive examination of possible intermolecular potentials. It appears from this and the work of others that a high-order agreement over a wide range of thermodynamic properties can only be possible by a more general potential function, or even preferably a potential in a numerical form. Table I lists the experimental P , V , T points of Crawford and Daniels⁸ taken along the melting curve of argon and some points of Witzenburg and Stryland⁹ along a high-pressure solid argon isotherm at 120.08°K near the melting curve. These data were used to choose a potential which would best reproduce the experimental pressures along the phase line. Two such potentials have the parameters $\alpha = 17$, $r^* = 3.775 \text{ \AA}$, $\epsilon/k = 120^\circ\text{K}$, and $\alpha = 15$, $r^* = 3.81 \text{ \AA}$, and $\epsilon/k = 126.9^\circ\text{K}$. The pressures calculated using these potentials in the LJD model are also shown in Table I. The fitting of the potential was done only to ensure that the model could reproduce the correct equation of state along the melting curve.

In fitting the intermolecular potential, we have specifically required the model to predict the pressure at the triple point to within ± 3 bars. This was done so that the $v_f^*(T_0, v_0)$ at the triple point could be used as the constant to determine the melting curve using Eq. (3). The melting curve was determined by finding for each T_m the volume v_m at which $v_f^*(T_m, v_m) = v_f^*(T_0, v_0)$. This then determines the T_m , v_m curve and it is possible to calculate all of the thermodynamic properties along this curve. The P_m , v_m , T_m results are shown in Figs. 1, 2, 4, and 5 where they are compared with the measurements of Crawford and Daniels. Also shown are the static P , V , T points in Table I that were calculated by the LJD model in obtaining the potential. Since the intermolecular potential used does not predict the experimental data exactly, these calculated values were also included in the figures to serve as a measure of the best agreement obtainable by the calculated melting curve. Figures 3 and 6 compare the P - T curves up to 420°K.

An inspection of the next to the last column in Table I shows that $v_f^*(T)/v_f^*(83.81)$ increases from 83.81°K to 108.12°K and then levels off, so it appears that the low-pressure melting region of argon might actually be somewhat anomalous. That this point is anomalous is borne out by the unusually high heat capacities and apparent vacancy formations or premelting¹⁰ that occur in this region.

In the belief that less vacancy formation would be present at the highest compressions, another melting curve was calculated by setting v_f^* at $T = 201.32^\circ\text{K}$ and $v = 21.69$ cc/mole equal to a constant along the melting curve, or

$$v_f^*(T_m, v_m)/v_f^*(201.32, 21.69) = 1.$$

TABLE I. Summary of experimental results and calculations to fit potential parameters.

T (°K)	V (cc/mole)	P_{expt} (kbar)	P_{LJD}^a (kbar)	$\frac{V_f^*(T)}{V_f^*(83.81)}^a$	P_{LJD}^b (kbar)
83.81	24.61	0.000	0.003	1.0000	0.000
94.73	24.34	0.451	0.443	1.0596	0.436
108.12	24.02	1.051	1.003	1.1184	0.991
120.85	23.65	1.674	1.621	1.1318	1.605
140.88	23.04	2.708	2.738	1.1141	2.711
160.40	22.54	3.805	3.881	1.1071	3.828
180.15	22.08	4.999	5.121	1.0969	5.029
201.32	21.69	6.335	6.421	1.1067	6.274
120.08 ^c	23.36	1.884	1.848		1.849
120.08 ^c	23.22	1.990	1.975		1.982
120.08 ^c	23.20	2.032	1.999		2.007

^aCalculations made with Eq. (5); $\alpha = 17$, $r^* = 3.775 \text{ \AA}$, $\epsilon/k = 120^\circ\text{K}$.

^bCalculations made with Eq. (5); $\alpha = 15$, $r^* = 3.81 \text{ \AA}$, $\epsilon/k = 126.9^\circ\text{K}$.

^cData of Witzenburg and Stryland (Ref. 9) taken along the 120.08°K isotherm. All other data are those of Crawford and Daniels (Ref. 8) taken along the melting curve.

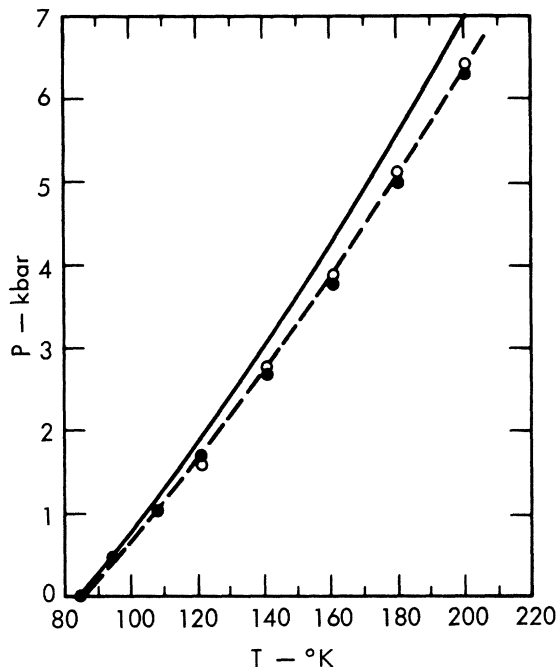


FIG. 1. Melting pressure versus melting temperature for argon, calculated for $\alpha = 17$; ●, data of Crawford and Daniels as listed in Table I; ○, LJD calculations listed in Table I. Solid curve, melting curve calculated by setting v_f^* (83.81, 24.61) to a constant. Dashed curve, melting curve calculated by setting v_f^* (201.32, 21.69) to a constant.

These results, also shown in Figs. 1-6, are clearly in excellent agreement with the experimental melting curves of Crawford and Daniels in the region of the phase diagram in which the potential has been determined. It is interesting to note that with v_f^* fixed at 201.32°K, a triple point of 86.8°K is predicted, which would point to a phenomenon leading to an effective premelting in argon. The disagreement at the high-pressure, high-temperature end of the P - T curve of Figs. 3 and 6 probably results because our potentials are not correct for these conditions, having been adjusted to predict lower-pressure, lower-temperature P , V , T points.

It should be noted that a potential may correctly predict the pressure but at the same time not correctly predict v_f^* . This is because the maximum contributions to the integrals occur at different regions of the potential. Consequently two potentials that predict almost identical P , V , T points may predict different melting curves. This is apparently so in the present case where the $\alpha = 17$ curve gives better agreement with the experimental melting curves. This difficulty is inherent in the use of a phenomenological potential for applications where the exact potential is not known.

Postulating that v_f^* is a constant along the melting curve is identical to assuming that the reduced free energy $A^*/kT = -\ln v_f^*$ is a constant. There are, of course, other possible reformulations of Lindemann's Law, such as reformulation in terms of the reduced entropy S^*/k , or the reduced energy E^*/kT , where

$$\frac{S^*}{k} = - \left(\frac{\partial A^*}{\partial T} \right)_v, \quad \text{and} \quad \frac{E^*}{k} = \left(\frac{\partial A^*}{\partial 1/T} \right)_v.$$

Calculations made assuming a constant reduced entropy give melting pressures differing by about 3% from the results for constant v_f^* , and poorer in agreement with experiment. These results are not shown. However, some calculations assuming that E^*/kT is a constant (shown in Fig. 3) are in poorest agreement. The present investigation is not so comprehensive nor so rigorous that it is possible to conclude that the first reformulation in terms of the partition function is superior to these two latter reformulations. This point is not pursued any further in this publication and we restrict ourselves to a literal reformulation in terms of the free volume.

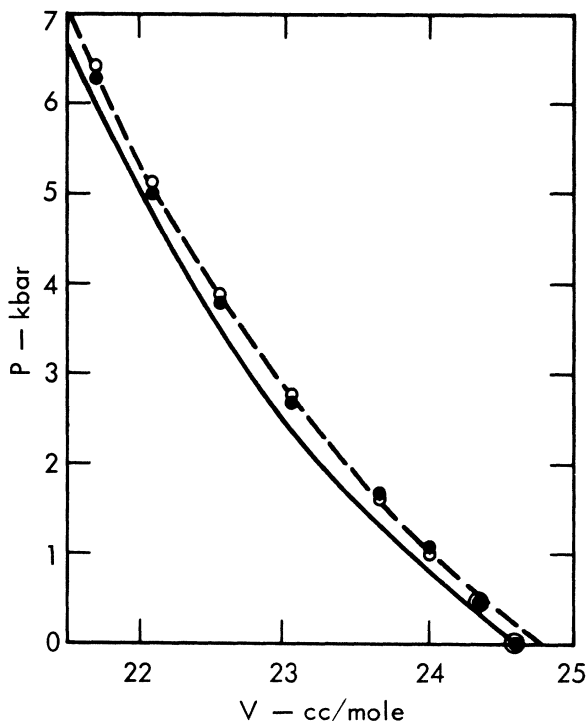


FIG. 2. Melting pressure versus melting volume for argon, calculated for $\alpha = 17$; ●, data of Crawford and Daniels as listed in Table I; ○, LJD calculations listed in Table I. Solid curve, melting curve calculated by setting v_f^* (83.81, 24.61) to a constant. Dashed curve, melting curve calculated by setting v_f^* (201.32, 21.69) to a constant.

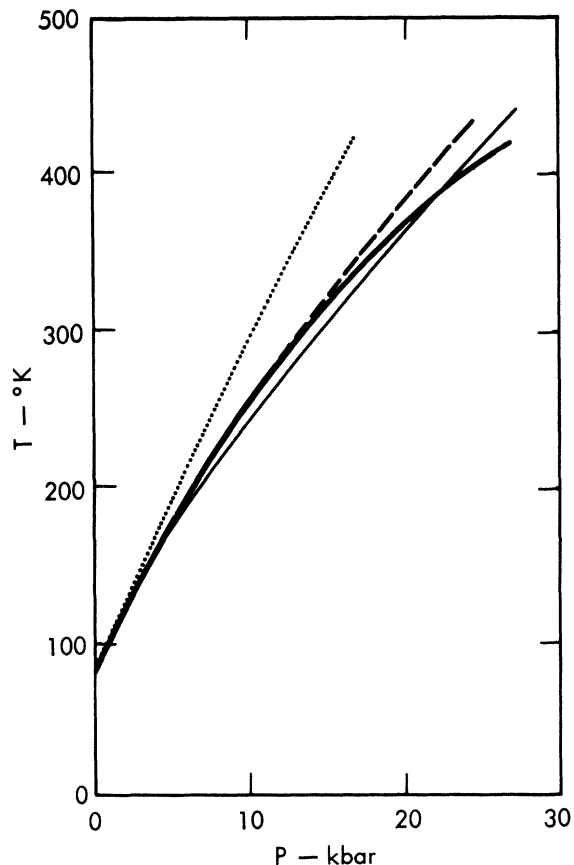


FIG. 3. Melting pressure versus melting temperature for argon up to 420°K, calculated for $\alpha = 17$. Bold solid curve, data of Lahr and Eversole (Ref. 11), and Grace and Kennedy (Ref. 12). Solid curve, melting curve calculated by setting v_f^* (83.81, 24.61) to a constant. Dashed curve, melting curve calculated by setting v_f^* (201.32, 21.69) to a constant. Dotted curve, melting curve calculated by setting E^*/kT (83.81, 24.61) to a constant.

IV. APPLICATIONS TO SIMPLE POTENTIAL FUNCTIONS

In this section, the generalized Lindemann principle is applied to some potential functions to derive a few well-known melting laws. In Sec. IV A it will be shown that for the Einstein oscillator, Eq. (3), leads immediately to Lindemann's Law as it should. In Secs. IV B and IV C, we derive forms of the Kraut-Kennedy melting law for two cases: IV B, systems in which the neighboring atoms interact via strong core-core repulsions and the force law is given by an inverse power repulsion, and IV C, systems in which core-core interactions are negligible and the properties of the system are determined primarily by the conduction-band electrons. In this case, recent

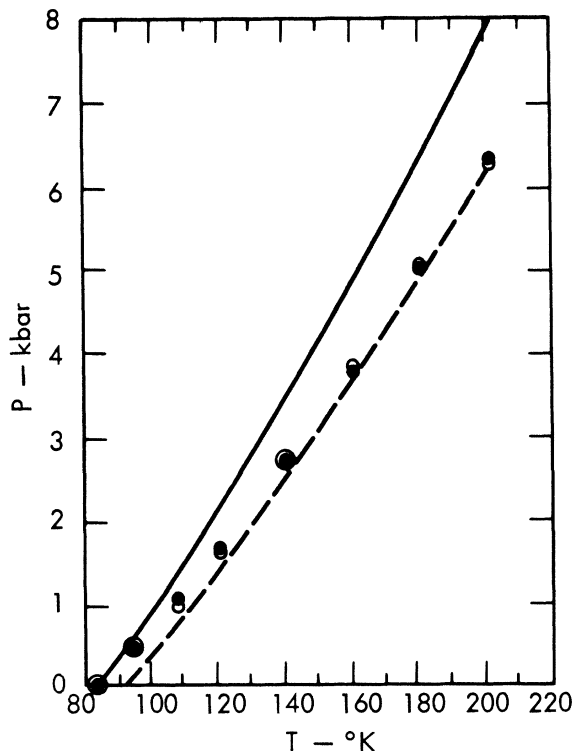


FIG. 4. Melting pressure versus melting temperature for argon, calculated for $\alpha = 15$; ●, data of Crawford and Daniels as listed in Table I; ○, LJD calculations listed in Table I. Solid curve, melting curve calculated by setting v_f^* (201.32, 21.69) to a constant. Dashed curve, melting curve calculated by setting v_f^* (201.32, 21.69) to a constant.

developments in the theory of metals show that we may treat such systems as hard spheres. In IV D, starting from this same generalized principle, we derive the Simon equation and illustrate its limitations.

A. Einstein Solid and Lindemann's Law

In the case for which the atom moves in an isotropic parabolic potential (Einstein solid) with force constant K ,

$$E(r) - E(0) = \frac{1}{2} Kr^2,$$

and in reduced coordinates as defined before

$$E(\lambda) - E(0) = \frac{1}{2} v^{2/3} K \lambda^2. \quad (6)$$

For Eq. (3) to remain a constant along the melting curve, it is necessary that at the melting volume V_m and melting temperature T_m

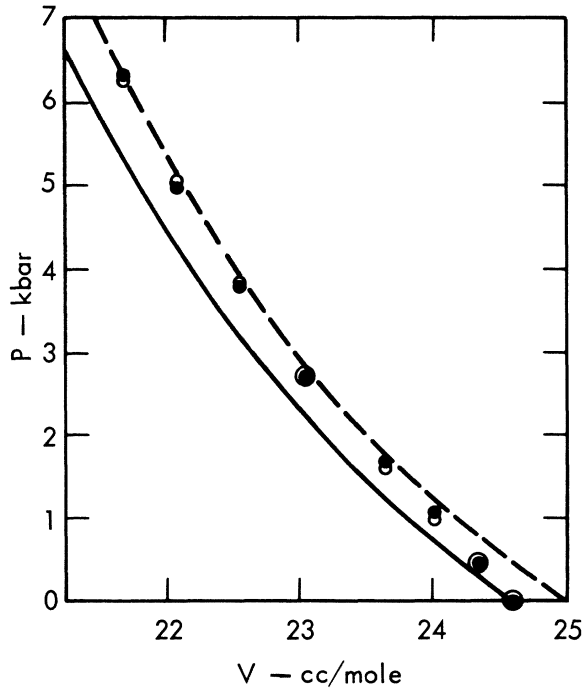


FIG. 5. Melting pressure versus melting volume for argon, calculated for $\alpha = 17$; ●, data of Crawford and Daniels as listed in Table I; ○, LJD calculations listed in Table I. Solid curve, melting curve calculated by setting v_f^* (83.81, 24.61) to a constant. Dashed curve, melting curve calculated by setting v_f^* (201.32, 21.69) to a constant.

$$v_f^* = 4\pi \int_0^1 \exp\left[-\left(\frac{V_m^{2/3} K}{2} - \frac{K}{kT}\right)\lambda^2\right] \lambda^2 d\lambda = \text{const},$$

which can be satisfied by

$$\frac{1}{2} V_m^{2/3} K / kT = \text{const} \quad (7)$$

and is Lindemann's Law.

B. For Atoms With Strong Core-Core Repulsions

If the atoms of the solid interact by pairwise additive repulsive forces of the inverse power form

$$\phi(r) = \epsilon (r^*/r)^n, \quad (8)$$

and the Z nearest neighbors surrounding an atom in its cage are considered to be smeared over that shell, then the potential in which the atom in the cell moves is given by^{4,6}

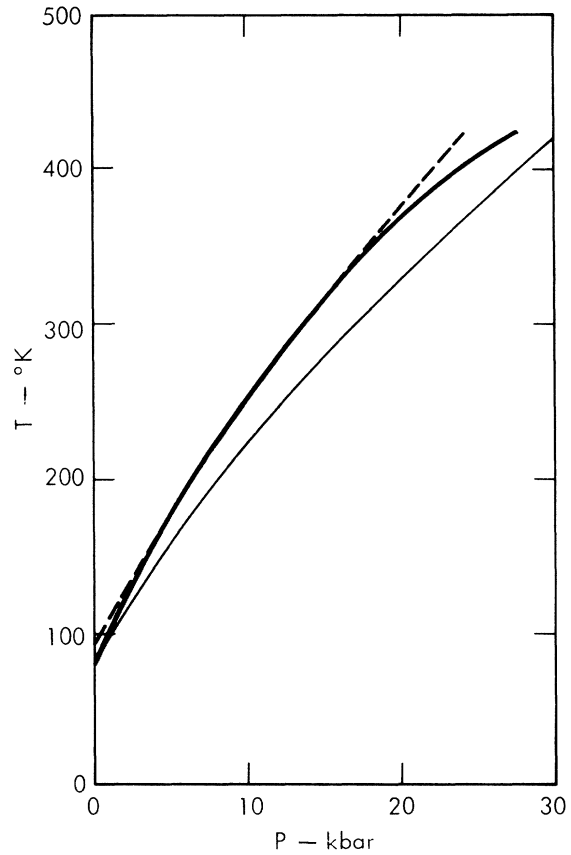


FIG. 6. Melting pressure versus melting temperature for argon up to 420°K, calculated for $\alpha = 15$. Bold solid curve, data of Lahr and Eversole (Ref. 11) and Grace and Kennedy (Ref. 12). Solid curve, melting curve calculated by setting v_f^* (83.81, 24.61) to a constant. Dashed curve, melting curve calculated by setting v_f^* (201.32, 21.69) to a constant.

$$E(\lambda) - E(0) = Z\epsilon (v^*/v)^{n/3} l(\lambda^2).$$

Here r^* , ϵ , and n are constants, and $v^* = r^{*3}/d$; d depends on the crystal structure, $l(\lambda^2)$ is a polynomial expansion in λ^2 and can be written in a closed form.

In the limit of the harmonic approximation, it can be shown that

$$E(\lambda) - E(0) = Z\epsilon (v^*/v)^{n/3} a_n \lambda^2, \quad (9)$$

where a_n is a constant depending on the crystal structure and the number of neighboring shells included. It should be noted that smearing the neighbors over a shell makes the potential field isotropic. Consequently, Eq. (9) differs from Eq. (6) only in that the force constant now has an explicit volume dependence.

To satisfy the melting condition of Eq. (3), it is necessary that

$$(Z\epsilon/kT_m)(v^*/v_m)^{n/3}a_n = \text{const.} \quad (10)$$

In what follows, T_0 and v_0 will refer to some standardized point along the melting curve, specifically the triple point unless otherwise stated.

Now

$$v_m = v_0 - \Delta v, \quad \text{where} \quad \Delta v = v_0 - v_m.$$

Substituting in Eq. (10), we get

$$\frac{Z\epsilon}{kT_m} \left[\frac{v^*}{v_0(1 - \Delta v/v_0)} \right]^{n/3} a_n = \text{const.}$$

We may evaluate the constant at $\Delta v = 0$ for which $T_m = T_0$ and $v_m = v_0$. Then

$$T/T_0 = (v_0/v_m)^{n/3} = (1 - \Delta v/v_0)^{n/3}. \quad (11)$$

This, when expanded, leads directly to a relationship [Eq. (12)] similar to the one proposed by Kraut and Kennedy, but containing higher-order terms:

$$\frac{T}{T_0} = 1 + \frac{1}{3}n \Delta v/v_0 + \frac{1}{3}n(\frac{1}{3}n + 1) \frac{1}{2}(\Delta v/v_0)^2 + \dots \quad (12)$$

The Kraut-Kennedy relationship is

$$T/T_0 = 1 + C \Delta v/v_0.$$

An inspection of the ratio of the quadratic to the linear term in Eq. (12) reveals that for any reasonable value of n , for example, $n = 9$, the quadratic term becomes 10% of the linear at $\Delta v/v_0$ of about 0.05. For transition metals such as iron and other substances in which core-core interactions are important, such as aluminum, zinc, and tin, the volume data do not extend to large compressions, so that Eq. (12) with higher-order terms neglected appears to be an adequate description of the Kraut-Kennedy law. However, the remarkable feature of the Kraut-Kennedy relationship is that the alkali metals obey the linear expression up to compressions of 0.4, wherein quadratic and higher terms, if present, should have begun to manifest themselves. Vaidya and Gopal¹³ attempted to derive the Kraut-Kennedy law by differentiating the Lindemann Law with respect to volume, using the Grüneisen hypothesis that the frequency spectrum of a solid depends only on the volume and then making a binomial expansion. They then obtained Eq. (11) where $\frac{1}{3}n$

$= 2(\gamma - \frac{1}{3})$ and γ is the Grüneisen parameter [see Eq. (15)]. However, these authors neglect the higher-order terms; this is incorrect for the alkali metals. These results indicate that any attempted derivation of the Kraut-Kennedy law starting from a harmonic-oscillator model must result in an expansion in $\Delta v/v_0$.

It is well known that at normal densities there is no appreciable core-core interaction in the alkali metals.¹⁴ Consequently Eq. (12), which is derived from a potential that is appropriate to a system in which strong core-core repulsions dominate, should not be applicable to the alkali metals. In Sec. IV C, we shall derive a melting law using a potential that is more appropriate to such systems.

C. For Alkali Metals (Hard Spheres)

In this section, we make use of some recent developments in the theory of metals. In particular, we draw heavily from the results of Ashcroft and co-workers.^{15,16} Ashcroft and Langreth calculated the ion-ion potential for a number of alkali metals and showed that these potentials to a good approximation may be represented by a hard-sphere potential. In this approximation, the ion may be thought of as moving through an electron fluid about its equilibrium position in a weakly varying potential to which it is confined by a steep repulsion. With this model Ashcroft has been able to successfully calculate the electrical resistivities of a number of alkali metals and their alloys. The model will be appropriate for the alkali metals as long as there are no strong core-core repulsions when the atoms are near their equilibrium positions. For this potential in the spherical-cell approximation, the free volume v_f of a hard-sphere solid is given by⁶

$$v_f = \frac{4}{3} \pi a^3 (1 - \sigma/a)^3,$$

where σ is the diameter of the hard-sphere atom, a is the nearest-neighbor separation, and $v = a^3 g$ where g depends on the crystal structure. In order for the melting criterion, Eq. (3), to apply, it must have at the melting temperature,

$$v_f/a^3 = \text{const, or } \sigma(T)^3/v_m = \text{const.} \quad (13)$$

This is Lindemann's Law for hard spheres, for which case it is exact. On the basis of their empirically determined σ (see below), Ashcroft and co-workers^{15,16} have shown that Eq. (13) with v_m equal to the volume of the liquid at melting holds for a number of alkali metals. They note that this "is a statement of Lindemann's melting law viewed from the liquid side of the phase transition." In Eq. (13), σ is a function of temperature because of the ability of the colliding atoms

to further interpenetrate at higher kinetic energies, and we will express this phenomenological character as

$$\sigma(T)^3 = -cT + b, \quad \text{where } c = -d(\sigma)^3/dT.$$

Substituting into Eq. (13)

$$(-cT_m + b)/v_m = \text{const.}$$

Using the properties at the triple point as was done in obtaining Eq. (11)

$$(-cT_m + b)/v_m = \sigma(T_0)^3/v_0,$$

$$T_m = [b - \sigma(T_0)^3]/c + (\Delta v/v_0)\sigma(T_0)^3/c.$$

Since $T_0[b - \sigma(T_0)^3]/c$,

$$\text{then } T/T_0 = 1 + (\Delta v/v_0)\sigma(T_0)^3/cT_0. \quad (14)$$

Equation (14) is identical to the Kraut-Kennedy melting law and $\sigma(T_0)^3/cT_0$ is equal to the constant C which has been determined from experiment for a number of substances as well as the alkali metals. In deriving Eq. (14), a number of approximations were made: (1) that a generalized Lindemann formulation is applicable, (2) that the interior potential can be approximated by a hard-sphere potential, and (3) that the hard-sphere volume decreases proportionally as the temperature. We will attempt to vindicate these approximations by calculating the Kraut-Kennedy law constant for the alkali metals.

Ashcroft and Lekner¹⁵ evaluated σ for the alkali metals in the liquid near the melting point by finding that value of σ at which the first peak of the hard-sphere liquid-structure factor agrees with the one experimentally determined from neutron-diffraction experiments. These authors also determined σ for sodium at a number of different temperatures from liquid compressibility data, so that it is possible to estimate $d\sigma^3/dT$ for Na. Also, for Rb, σ was estimated from neutron-diffraction experiments at a number of different temperatures by determining the σ which gives the correct height of the structure factor. From these numbers we calculated $d\sigma^3/dT$ for Rb. In the spirit of the hard-sphere model, we assume that the hard-sphere radii are only functions of temperature, and the values determined by Ashcroft and Lekner for the liquid near the melting point will be used in the solid at the melting point to calculate the melting-law constant in Eq. (14). To circumvent the lack of temperature-dependent experimental data for Li and K, $d\sigma^3/dT$ was estimated for these materials by assuming that $d\sigma^3/dT$ varies linearly with σ^3 , interpolating for K, and extrapolating for Li. The results (Table II)

TABLE II. Summary of calculations of melting-law constant using hard-sphere data of Ashcroft and Lekner (see Ref. 15). Values in parentheses were estimated as discussed in the text.

	T_0 (°K)	σ^3 (Å ³)	$10^2 \frac{d\sigma^3}{dT}$	C_{theoret}	C_{expt}
Li	453	19.68	(-1.24)	3.5	1.3
Na	373	35.29	-1.59	6.0	6.3
K	338	67.40	(-2.32)	8.6	8.7
Rb	313	79.51	-2.71	9.4	13.2

are in good agreement with the experimentally determined values. While in absolute terms the agreement ranges from very good in the case of Na and K to poor in Li and fair in Rb, the overall agreement and the correct qualitative trend in this group of elements does appear to vindicate the approximations that have been made. Because no volumes are known along the curve, Kraut and Kennedy in applying their relationship to experiment use as the melting volumes the volumes for the solids at 25°C measured by Bridgman that are at the same pressure as at the melting temperature. Consequently, the agreement between theory and experiment must be considered satisfactory.

Equations (7), (11), and (14) were all derived from a generalized Lindemann point of view, and consequently all are equivalent models of melting, differing only because of the form of the potential field in which the atom wanders. For metals in which the free-electron character dominates, Eq. (14) is correct provided that there are no strong core-core interactions between the ions. At compressions at which these interactions are no longer negligible and the neighboring cores strongly repel one another, then Eq. (12) is a more appropriate form of the melting law, and the melting-law constant is directly related to the power of the repulsive parameter. Since this will be the case at some compression for all substances, then Eq. (11) correctly predicts that the melting temperature will become unbounded as the melting volume goes to zero and no solid-to-fluid critical point will exist.

D. Simon Melting Law

The Lindemann Law and the Kraut-Kennedy law relate the melting volume and the melting temperature via some intermediate parameters. In this section we again demonstrate one of the advantages of reformulating the Lindemann principle in terms of the partition function by straightforwardly deriving a relationship between pressure and temperature and show that it leads to a form of the Simon equation.

Using the potential function [Eq. (9)], and differentiating Eq. (4) with respect to volume, we obtain an expression for pressure

$$P = P(0, v) + (3kT/v) \left(\frac{1}{6} n + \frac{1}{3} \right), \quad (15)$$

where $P(0, v)$ is the pressure at 0°K and volume v .

The term in brackets is a constant and is the Grüneisen parameter γ for this model. Equation (15) is an equation of state and only relates the allowable values of P , V , and T . To get the melting conditions or the allowable P , V , T along the melting curve, we must impose the melting condition that $v_f^* = \text{const}$. This condition is equivalent to requiring that Eq. (11) be obeyed.

Substituting Eq. (11) into Eq. (15), we get

$$P_m = P(0, v_m) + \frac{3kT_0}{v_0} \left(\frac{T_m}{T_0} \right)^{1+3/n} \left(\frac{n}{6} + \frac{1}{3} \right), \quad (16)$$

which may be rewritten

$$P_m = P(0, v_m) + a \left(T_m/T_0 \right)^d, \quad (17)$$

where $d = 1 + 3/n$; $a = 3(kT_0/v_0)(n/6 + 1/3)$ and n are constants. Equation (17) can be recognized as the Simon equation. In the application of the Simon equation to experimental data, $P(0, v_m)$ is always taken as a constant, and it is for this reason that the equation has apparently proven unreliable when extended to large pressures.

The Simon equation was originally proposed on empirical grounds and later derived by Salter.¹⁷ Salter combined the Grüneisen equation of state with Lindemann's Law, then assumed γ and $P(0, v_m)$ to be constants for all volumes and arrived at Simon's equation. His derivation is equivalent to starting with Eq. (6) rather than Eq. (9). The results of calculations from Sec. III

illustrate why the Simon equation fails. For the $\alpha = 17$ potential with v_f^* set to a constant for $T = 201.32^\circ\text{K}$, γ and $P(0, v_m)$ were calculated in Sec. III by the LJD cell model along with the melting curve from the triple point (83.81°K) up to 420°K . The total variation of $P(0, v_m)$ over this range is 11.6 kbar, while the total pressure variation is only 26 kbar. The calculated γ changes by about 25%. Obviously these terms cannot be taken as constants. At higher pressure $P(0, v_m)$ will rise even more sharply with compression. Consequently the Simon equation as generally applied cannot be extrapolated with any confidence.

V. DISCUSSION

What we have tried to do in this paper is to show how the Lindemann point of view of melting may be generalized so that it is applicable to any intermolecular potential and not only to the harmonic-oscillator form. The application to solid argon results in a melting curve which is in good agreement with experiment. This reformulation also provides a unifying framework which facilitates the theoretical derivation of other melting laws such as the Kraut-Kennedy law and the Simon equation. It has been possible to show that these laws follow directly from the Lindemann point of view and also to show their limitations. These results appear to further justify the Lindemann approach and also to suggest that, since the arrangement of the atoms in space is the central feature in melting and the criteria for melting may be established by only considering one phase, then the melting problem is essentially a packing problem, the essence of which is contained within the hard-sphere melting results.¹⁸

ACKNOWLEDGMENT

I wish to thank Dr. William Hoover for having read the manuscript and for many enlightening discussions.

*Work performed under the auspices of the U. S. Atomic Energy Commission.

¹F. A. Lindemann, *Z. Physik* **11**, 609 (1910).

²F. E. Simon and G. Glatzel, *Z. Anorg. Allgem. Chem.* **178**, 309 (1929).

³E. A. Kraut and G. C. Kennedy, *Phys. Rev.* **151**, 668 (1966).

⁴T. L. Hill, *An Introduction to Statistical Thermodynamics* (Addison-Wesely Publishing Co., Inc., Reading, Mass., 1960).

⁵J. E. Lennard-Jones and A. F. Devonshire, *Proc. Roy. Soc. (London)* **A163**, 53 (1937); **A165**, 1 (1938).

⁶J. A. Barker, *Lattice Theories of the Liquid State* (The Macmillan Co., New York, 1963).

⁷M. Ross and B. Alder, *J. Chem. Phys.* **46**, 4203

(1967).

⁸R. K. Crawford and W. B. Daniels, *Phys. Rev. Letters* **21**, 367 (1968).

⁹W. van Witzenburg and J. C. Stryland, *Can. J. Phys.* **46**, 811 (1968).

¹⁰A. J. E. Foreman and A. B. Lidiard, *Phil. Mag.* **8**, 97 (1963); R. H. Beaumont, H. Chilhara, and J. A. Morrison, *Proc. Phys. Soc. (London)* **78**, 1462 (1961).

¹¹P. H. Lahr and W. G. Eversole, *J. Chem. Eng. Data* **7**, 43 (1962).

¹²J. D. Grace and G. C. Kennedy, *J. Phys. Chem. Solids* **28**, 977 (1967).

¹³S. N. Vaidya, and E. S. R. Gopal, *Phys. Rev. Letters* **17**, 635 (1966).

¹⁴E. B. Royce, *Phys. Rev.* **164**, 929 (1967).

¹⁵N. W. Ashcroft and J. Lekner, Phys. Rev. 145, 83 (1966).

¹⁶N. W. Ashcroft and D. C. Langreth, Phys. Rev. 159, 500 (1967).

¹⁷L. Salter, Phil. Mag. 45, 369 (1954).

¹⁸B. J. Alder and T. E. Wainwright, J. Chem. Phys. 33, 1439 (1960).

PHYSICAL REVIEW

VOLUME 184, NUMBER 1

5 AUGUST 1969

COMMENTS AND ADDENDA

The Comments and Addenda section is for short communications which are not of such urgency as to justify publication in Physical Review Letters and are not appropriate for regular Articles. It includes only the following types of communications: (1) comments on papers previously published in The Physical Review or Physical Review Letters; (2) addenda to papers previously published in The Physical Review or Physical Review Letters, in which the additional information can be presented without the need for writing a complete article. Manuscripts intended for this section may be accompanied by a brief abstract for information-retrieval purposes. Accepted manuscripts will follow the same publication schedule as articles in this journal, and galley proofs will be sent to authors.

Electron-Impact Ionization Cross Section of Ions

K. C. Mathur, A. N. Tripathi, and S. K. Joshi

Physics Department, University of Roorkee, Roorkee, India

(Received 24 February 1969; revised manuscript received 22 April 1969)

A comparative study has been made of the ionization cross section of ions Li^+ , Na^+ , K^+ , Rb^+ , Cs^+ , Ne^+ , N^+ , and Mg^+ using different velocity distribution functions for the atomic electrons in classical impulse approximation. The results are discussed in the light of the available experimental and theoretical results.

1. INTRODUCTION

The problem of the theoretical treatment of electron-impact ionization of neutral atoms has received much interest.¹ The simple classical binary encounter model^{2,3} provides a simple framework for estimating ionization cross sections of atoms which turn out to be reliable specially at high energies and reasonable for almost all incident energies. However, not many attempts have been made for the calculation of ionization cross section of ions by electron impact. In the case of ions, the problem becomes com-

plicated, because of the effects of the residual ionic field. Very recently, Thomas and Garcia⁴ obtained a model solution within the framework of binary encounter theory in which the effect of residual ionic field was explicitly taken into account. We have used the model of Thomas and Garcia to calculate the cross sections for the ionization of the ions Li^+ , Na^+ , K^+ , Rb^+ , Cs^+ , Ne^+ , N^+ , and Mg^+ . We have studied the use of δ -function distribution function, and in two cases the use of a quantal momentum distribution function for the bound electrons.

2. THEORY

Thomas and Garcia studied a model in which they consider the impact of an electron of kinetic energy E_1 on a fixed ion of net charge Z' . The incident electron undergoes a binary collision with the bound electron of energy U , at a distance ξ from the nucleus and results in an energy transfer $\Delta E \geq U$. The kinetic energy of the incident electron at the collision radius ξ is $E_1' = E_1 + Z'/\xi \geq E_1$. The cross section for the ionization of the ion is given by

$$\Sigma = \frac{1}{4} \Sigma' \left(1 + \left\{ 1 + \frac{2Z'\pi}{\beta_1 \Sigma'} \left[\frac{Z'}{\beta_1 - \beta_1} - \left(\frac{Z'^2}{(\beta_1 - \beta_1)^2} - \frac{\Sigma'}{\pi} \right)^{1/2} \right] \right\}^{1/2} \right)^2, \quad \beta_1 = \frac{E_1}{U}, \quad \beta_1' = \frac{E_1'}{U}. \quad (1)$$

Here the factor in parentheses represents the magnification of the cross section due to the curvature of